A smart Method for Multi-zonal Virtual Power Plant Scheduling with Presence of Electric Vehicles

Zahra Moravej, Saeid Molaei, Alireza Jodaei

Abstract— Microgrids are practical view of integration of distributed generations (DGs) into distribution systems. In this regard, utilizing appropriate technologies and accurate recognition of energy generation and storage systems, as well as optimal scheduling for these resources are of the paramount importance in microgrids. Therefore, connection of DG resources and storages to the grid in the form of virtual power plant in order to increase efficiency and owners' interest has attracted significant attention of researchers and distribution network operators. This research presents a model for optimal day-ahead scheduling of heat-power generation units in a multi-zonal virtual power plant (VPP). This VPP includes a number of combined heat-power generations, distribution network loads, and electrical vehicles with smart charging as well as energy storages. In order to approach reality of distribution systems, uncertainty related to behavior of electrical vehicles was modeled with Monte Carlo simulation while uncertainties of generation and electrical/thermal loads were modeled using a probabilistic method. Matlab software and swarm robotics search & rescue (SRSR) has been used as an optimization tool in this paper. Results confirmed the effectiveness of the proposed method.

Keywords— renewable energy sources, energy storage, combined heat and power generation, virtual power plant, load uncertainty, electric vehicles.

I. INTRODUCTION

Smart grids' utilization has experienced a remarkable increase in power grids; meanwhile, virtual power plants (VPPs) have been promising tools to promote effective penetration of distributed generations (DGs) and energy storage devices in microgrids. To provide continuity of balancing demand and generation, renewable sources will be more active than today in near future due to the tendency of massive investment on renewable energy sources (RESs) by countries. However, due to the uncertain and intermittent nature of RESs, RESs would create problems on power system operations such as power quality, efficiency, stability and reliability. Owing to having problems with RESs integration, virtual power plant (VPP) has introduced to make this integration smooth without compromising the grid stability and reliability along with offering many other techno economic benefits [1].

In addition, VPPs, while working under supervision of a generation coordinating unit, are strongly effective tools, allowing consumers to respond to load management signals. Load response can be economically beneficial both for distributed energy resources (DERs) and the power grid itself [2],[3]. A large number of researches carried out in this field reflect the great attention of researchers to VPPs. Recently, the idea of VPPs is extended to various generation resources like renewable energy sources (RESs), combined heat and power plants (CHPs), as well as controllable loads and energy storage systems when acting as a unified power plant [4],[5].

In smart-grid framework, VPPs allow small plant owners to access energy market in a "collective" form to compensate for unanticipated power fluctuations due to wind farm and solar energy utilization via coordinated operation of small power plants [6]. Management systems of generation scheduling coordination are the central core of a VPP, which communicate using a communication infrastructure for data exchange [7]. Scheduling of generating units receive signals from power farms (wind and solar) and market. This schedules and operates generation power of each energy source which is done regarding to market price signals, energy demand, wind speed, and sunlight intensity. It takes into account the current energy level of energy storage devices as well [8].

A new concept of VPP is presented in [6], taking into account energy storages, CHP systems, RESs, responsive loads, and also various forms of micro-generators as well as conventional power plants. Based on this initial design, all resources belonging to a given company exchange power with utility from a common coupling point (CCP). In [9], authors built a CHP dispatch model for wind-CHP system with solid heat storage device aiming at minimizing system coal consumption, and set system demand-supply balance and units' operation conditions as the operation constraints. Furthermore, robust stochastic optimization theory has been utilized to describe wind power output uncertainty in a small-scale VPP.

Recently, especially in [10], a new and challenging model for VPP in the form of large-scale virtual power plant (LSVPP) has been proposed and studied. In the mentioned research, various power generators, storages and load sources are distributed in a vast geographical area, while each of them has their own special coupling point to utility. In [11], a bi-level scheduling approach for VPPs and intermittent renewable DGs with a large number of distributed thermostatically controlled loads is presented to diminish the net exchange power deviation caused by the

Z. Moravej, Faculty of Electrical and Computer Engineering Semnan University, Semnan, Iran (e-mail: zmoravej@semnan.ac.ir).

S. Molaei, Faculty of Electrical and Computer Engineering, Semnan University, Semnan, Iran (e-mail: s_molaei@semnan.ac.ir).

A. Jodaei, Faculty of Electrical and Computer Engineering Semnan University, Semnan, Iran (e-mail: a.jodaei@semnan.ac.ir).

forecast error of renewable energy. Similar problems have been solved in [12] using linear programming and in [13] using stochastic programming. It should be noted that grid limitations are not considered in [12]; also there is no possibility for load reduction scheduling. However, the case study in this paper is a system which includes only one thermal power plant and two renewable energy sources with one common coupling point to utility. In [14], the same authors have presented another case study, in which focus is on minimizing operation costs instead of maximizing profit. Other papers have considered different time horizons and time steps using linear programming. In this regard, [15] has focused on optimal strategies of load control in real time, while [6] has regarded only annual average of parameters (costs, prices, and energy generation) in order to determine optimal annual planning. Authors in [6] have presented a developed version of their algorithm with goal of determining optimal storage capacity in VPP, taking into account sensitivity analysis for price parameters in [8]. Concept of VPP regional control has been well described in [13] and [15], but presence of RESs has been overlooked in these works. Also, model of thermal power plants in mentioned works is very simple, since plant minimum power is not taken into consideration, leading to over-simplification of power plants' contribution problem. In [16] utilizing large number of DERs in a VPP in order to generate and market both thermal and electrical energy is proposed, however only thermal storage was considered in case studies and price of energy and fuel has been assumed to be constant.

The ultimate goal in [17] to determine the active demand power required to increase system loading capability and to withstand disturbances. The effect of different types of DG units in simulations is considered and then the efficiency of each equipment such as converters, wind turbines, electrolyzes, etc., is achieved to minimize the total operation cost and losses, improve voltage profiles, and address other security issues and reliability. The simulations are done in three cases and compared with HOMER software to validate the ability of proposed model.

On the other hand, decreased dependency on fossil fuels and reduced pollution are among the reasons for growing use of electric vehicles (EVs) in personal transportation. In this regard, plug-in hybrid EVs (PHEVs) has attracted many researchers, so that in many researches EVs are present in VPPs. In [18], an analytic based investigation on comparison between utilization of bulk electrical storages and EVs for a VPP has been accomplished. In other words, these technologies have been compared in terms of business incentives and technical performance. In [19], a VPP model with EVs and wind turbines in LSVPPs has been considered. EV behavior has been simulated with Monte Carlo model. Modeling is done on a 118-bus network where operation costs and pollution emission were considered as the objective functions. In [20], a stochastic programming for VPP with presence of wind units, solar units, and EVs has been presented, taking into account uncertainty. In this work, enhanced particle swarm optimization algorithm with fuzzy rules has been used for optimization, and multi-objective function including optimization cost and network reliability has been evaluated. In [21], a new method of VPP operation was proposed for taking part in day-ahead energy market. Uncertainty in generation, consumption, and prices was modeled using a stochastic method. Monte Carlo simulation was also considered in this work in order to model vehicle random behavior. Presence of EVs in a VPP in order to provide reserve has been modeled in [22]. In this paper, programming was performed so that EVs will be charged when energy exceeds consumption and will be discharged as reserves in overload time. In [23], it was shown that how generation scheduling coordination unit can manage its energy resources in order to maximize aggregate daily profit (regarding buy and sell price).

This research presents a new algorithm for VPP scheduling optimization which simultaneously executes schedule for generation unit contribution, thermal and electrical storages, EVs, and load flow. Although there have been some efforts in previous researches [10]-[15] on LSVPPs, none of them have considered the following items simultaneously, which will be addressed in this work:

1. Thermal aspects: local thermal loads, CHP units and thermal power plant requirements.
2. Energy storage devices (both electrical and thermal).
3. Taking into account EVs in a LSVPP with smart charge/discharge.
4. Considering consumer uncertainty in the form of a statistical method.

Unlike [12] and [13], main focuses in [23] is optimization, providing a general schedule for LSVPPs while system limitations are present. In this research a regional scheduling algorithm for VPPs is proposed taking into account consumer uncertainty. An evolutionary algorithm has been used during the simulations in order to examine the network in grid-connected and islanded modes.

II. Problem Formulation and Unit Scheduling

In this work, a group of VPPs were connected to a general distribution network. Structural properties of elements in the network including active source and storage capacity had been determined in previous stages and might not change during the operation.

A. Topology and model of VPPs

VPPs studied in this work were a complex of a generation system connected to a radial general network separately and fed through a sub-bus. Each VPP was modeled as shown in

Fig. 1. Economic profit and associated transactions of each load and generation resource were not taken into account separately within each VPP; consequently, LSVPP optimization was considered as shown in

Fig. 2. In this network, only active power of elements was investigated and reactive power and transmission line losses were overlooked.

One of the important and emphasized points in this research compared to previous ones, like [6], [8], [23], [24] is that in this work only one VPP will not be investigated; but each VPP is just an element of a larger network (LSVPP). Therefore, using expressions proposed in [10], the present work focuses on a LSVPP, regarding the real location of each RES in network. Thermal section of the model connected to right side of the bus

is a certain load which can be fed using CHP, boiler or thermal storage device.

If thermal generation of a CHP exceeding network thermal demand is not absorbed via thermal storage element because of energy and/or power limitations, the surplus thermal energy (P_{sur}) will be released using a thermal converter. It should be noted that both CHP and boiler are gas-fired. Electrical section of the network is divided into two sub-sections; the first sub-section is called internal part, including an automatic conventional generator, the boundary of which is PCC_i. This part of the model, which regarding

Fig. 1 connects to the left side of bus, mainly consists of an electrical consumer which can be fed via a CHP, an internal RES, and/or an electrical storage device. The Second sub-section includes an external RES which is able to sell energy to network or internal part.

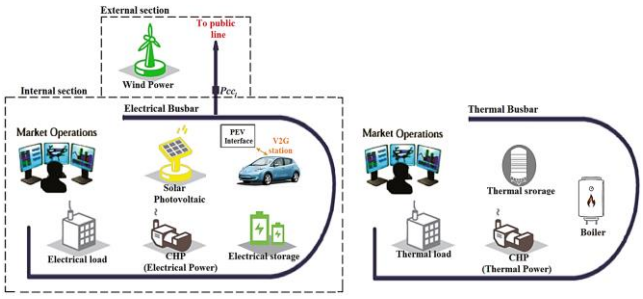

Fig. 1. A single VPP structure

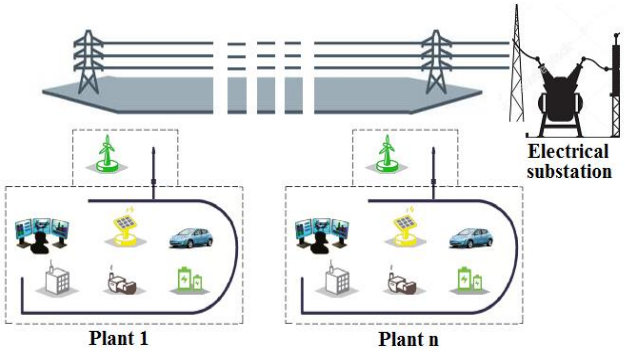

Fig. 2. General network including n VPPs

B. Optimization Problem Structure

The proposed algorithm was executed in one hour steps. Daily optimal operation algorithm was determined for the dispatchable generation resources (boilers, CHPs, conventional power plants) and energy storage devices. This work aims at meeting thermal and electrical loads as well as maximizing daily net benefit of VPP. Also this algorithm was designed so as to allow load shedding and/or RES limitation in case of severe shortage in transmission line capacity during LSVPP islanded operation.

a) Restructured systems' tariff

In order to form tariff for restructured systems, following pricing mechanism is applied.

1. Energy sales tariff: when internal generated power (P_{int}) is positive i.e. it sales energy to upstream network as well as it meets the internal demand, in addition to the main sold energy price, it deserves an extra earning as encouraging tariff [25].
2. Fuel purchase tariff (generally natural gas): In case of CHPs, regardless of type of consumption, to generate either heat or electricity, a combination of the two prices is considered as an encouraging tariff [25].
3. Incentive plan for RESs: It is an extra payment to the total generated power, either consumed internally or sold to upstream network.

C. Mathematical model

a) CHP

Electrical to thermal power conversion rate (λ) is considered as a constant factor in this system.

$$P^{s}_{tch,pt} = \lambda_{chp,p}.P^{s}_{echp,pt} \quad (1)$$

As shown in Eq. (2), the CHP power output is either zero or a value between minimum technical power and nominal power.

$$P_{echp-\min,pt}.U^{s}_{chp,pt} \le P^{s}_{echp,pt} \le P_{echp-\max,pt}.U^{s}_{chp,pt} \quad (2)$$

where, $U^{s}_{chp,pt}$ indicates on/ off state of the units.

b) Thermal and electrical storage device

One of the main capabilities of the proposed algorithm is optimizing thermal and electrical storage devices' energy level in each stage of time. Equations (3) and (4) state power limits during charge/discharge for electrical and thermal storage devices, respectively.

$$-P_{es-char,p} \le P^{s}_{es,pt} \le P_{es-disc,p} \quad (3)$$

$$-P_{ts-char,p} \le P^{s}_{ts,pt} \le P_{ts-disc,p} \quad (4)$$

Each thermal or electrical storage device can be modeled via applying related minimum and maximum allowable energy levels. Batteries' depth of discharge (DoD) has direct effect on their life span [26]. Equations (5) and (6) refer to lower and higher limits of electrical storage energies, respectively.

$$\frac{\left(e_{es-start,p} - e_{es-\max,p}\right)}{\delta} \le \eta_{es,p} \sum_{\substack{i=Ts \\ \text{char}}}^{t} P^{s}_{es,pi} + \sum_{\substack{i=Ts \\ \text{dischar}}}^{t} P^{s}_{es,pi} \quad (5)$$

$$\eta_{es,p} \sum_{\substack{i=Ts \\ \text{char}}}^{t} P^{s}_{es,pi} + \sum_{\substack{i=Ts \\ \text{dischar}}}^{t} P^{s}_{es,pi} \le \frac{\left(e_{es-start,p} - e_{es-\min,p}\right)}{\delta} \quad (6)$$

Equations (7) and (8) are related to thermal storage devices. In order to include energy efficiency in operation cycle, charge and discharge stages were considered completely separate.

$$\frac{\left(e_{ts-start,p} - e_{ts-\max,p}\right)}{\delta} \le \eta_{ts,p} \sum_{\substack{i=Ts \\ \text{char}}}^{Te} P^{s}_{ts,pi} + \sum_{\substack{i=Ts \\ \text{dischar}}}^{Te} P^{s}_{ts,pi} \quad (7)$$

$$\eta_{ts,p} \sum_{\substack{i=Ts \\ \text{charg}}}^{Te} P^{s}_{ts,pi} + \sum_{\substack{i=Ts \\ \text{dischar}}}^{Te} P^{s}_{ts,pi} \le \frac{\left(e_{ts-start,p} - e_{ts-\min,p}\right)}{\delta} \quad (8)$$

Ts and Te are start and end time of simulation, respectively. At the end of simulation period, initial energy level in all storages should be equal to one at the beginning of operation period:

$$\eta_{es,p} \sum_{\substack{i=Ts \\ \text{char}}}^{Te} P^{s}_{es,pi} + \sum_{\substack{i=Ts \\ \text{dischar}}}^{Te} P^{s}_{es,pi} = 0 \quad (9)$$

$$\eta_{ts,p} \sum_{\substack{i=Ts \\ \text{char}}}^{Te} P^{s}_{ts,pi} + \sum_{\substack{i=Ts \\ \text{dischar}}}^{Te} P^{s}_{ts,pi} = 0 \quad (10)$$

If final energy level at the end of operation period differs from initial value, for instance, when simulation algorithm is applied for less than 24 hours, previous equations will change to following ones:

$$\eta_{es,p} \sum_{\substack{i=Ts \\ \text{char}}}^{Te} P^{s}_{es,pi} + \sum_{\substack{i=Ts \\ \text{dischar}}}^{Te} P^{s}_{es,pi} = \frac{\left(e_{es-start,p} - e_{es-final,p}\right)}{\delta} \quad (11)$$

$$\eta_{ts,p} \sum_{\substack{i=Ts \\ \text{char}}}^{Te} P^{s}_{ts,pi} + \sum_{\substack{i=Ts \\ \text{dischar}}}^{Te} P^{s}_{ts,pi} = \frac{\left(e_{ts-start,p} - e_{ts-final,p}\right)}{\delta} \quad (12)$$

c) Internal and external RESs

Internal and external RESs' generated power can be limited regarding predicted solar and wind powers:

$$0 \le P^{s}_{ires,pt} \le P_{ires-\max,pt} \quad (13)$$

$$0 \le P^{s}_{eres,pt} \le P_{eres-\max,pt} \quad (14)$$

Since generated power via RESs is presented into market with the highest prices, limiting generated power and not using RESs' maximum generated power is not economical, as the goal is to maximize VPP earning (in objective function). To this aim, optimization algorithm disconnects RESs only in conditions where either generation exceeds demand or network faces high congestion.

d) Boiler

A boiler becomes active when CHP is not able to respond fully to the thermal load. If fuel price changes during the day, algorithm is capable of recognizing operation strategies in order to avoid using boiler. This is one of the capabilities of proposed method compared to those of previous researches regarding VPPs [16]. Thermal power provided by boiler should remain in its capacity limits:

$$0 \le P^{s}_{boil,pt} \le P_{boil-\max,pt} \quad (15)$$

e) Load shedding

When it is not possible to respond to demand fully, because of severe network limitations and lack of internal generation, a deliberate load shedding limited to utmost γ, is planned by limiting a part of electrical power demand.

$$0 \le P^{s}_{sens,pt} \le \gamma_{el,pt} \quad (16)$$

f) NETWORK OBJECTIVES

Current in all transmission lines should not pass the allowable thermal limit:

$$\left|P^{s}_{lin,pt}\right| \le P_{lin-\max,pt} \quad (17)$$

Network radial topology allows simple power flow calculation starting from first unit in

Fig. 2. If the algorithm is executed in islanded operation, allowable power for the last line connected to substation is set zero:

$$P_{lin,Npt} = 0 \quad (18)$$

g) EV charging behavior

PHEV charging behavior is influenced by various factors including charging strategy, number of PHEVs being charged at the same time, charging type, battery state of charge (SOC), capacity, charging start time, and charging time duration. In this research, a smart strategy was considered for vehicle charging; this means PHEVs would not necessarily be charged at any hour they are connected to charging plugs. Main idea beyond all smart charging strategies is that vehicles be charged when it has maximum benefit both for vehicle owner and for network operator. A normal distribution function is proposed as follows in order to indicate complexity of using different smart charging programs and charging start time [27]:

$$f(t_{start}) = \frac{1}{\sigma\sqrt{2\pi}} e^{\left(-0.5\left(\frac{t_{start}-\mu}{\sigma}\right)^2\right)} \quad \mu=1,\ \sigma=3 \quad (19)$$

Remaining charge state of battery is calculated from travelled distance by vehicle. It should be noted that travelled distance by a vehicle is presented as a logarithmic probability distribution function [28]. Therefore, battery SOC is calculated using vehicle travelled distance and its all-electric range (AER):

$$SOC = \begin{cases} 0 & m > AER \\ \dfrac{AER - m}{AER} \times 100\% & m \le AER \end{cases} \quad (20)$$

Various types of PHEVs are available based on their AER, e.g. PHEV-20, PHEV-30, PHEV-40, PHEV-60 where the number indicates PHEV AER in terms of miles. In this research, PHEV-20 was considered as it has been proven during a long time that it has high usage potential in the market [29]; however, the proposed method is general and other types of PHEVs can be replaced. Charging time of PHEVs is calculated by the following formula:

$$t_D = \frac{C_{bat} \times (1 - SOC) \times DOD}{\eta \times P} \quad (21)$$

It should be noted when PHEVs reach house, depending on vehicle's need and regarding maximum DoD limits, (reported as 80% [29]) charging starts, but charging duration is limited by both charger performance level (p) and charger efficiency (η). Charging rate, as shown in Table 1, is determined by the charging level of charger. Level 1 and 2 are mainly used for PHEVs capable of being connected at house. Level 3 was not considered in this research, since it is used for public and commercial transportation. In addition, battery capacity distribution (C_{bat}) in a given range for each class, considered as

a normal probability distribution in [28], is as follows:

$$\mu_{C_{bat}} = \frac{MinC_{bat} + MaxC_{bat}}{2}$$
$$\sigma_{C_{bat}} = \frac{MaxC_{bat} - MinC_{bat}}{4} \quad (22)$$

Table 1. Various types of PHEV charger

Charger type	Input voltage	Max. Power (Kw)
Level 1	VAC 120	1.44
Level 2	208-240 VAC	11.5
Level 3	208-240 VAC	96
Level 4 (DC)	208- 600 VDC	240

h) Thermal and electrical power balance

Regarding Fig. 1 and equations (24) and (25), power balance in internal and external buses would be as follows:

$$P^s_{\text{int},pt} = P^s_{echp,pt} + P^s_{ires,pt} + P^s_{es,pt} + P^s_{eens,pt} + P^s_{PHEV,pt} - P^s_{el,pt} \quad (23)$$

$$P^s_{lin,\text{N}\,pt} = P^s_{\text{int},pt} + P^s_{eres,pt} + \sum_{i=1}^{p-1}\left(P^s_{\text{int},it} + P^s_{eres,it}\right) \quad (24)$$

In previous equations, power flow calculation starts from VPP unit number 1. Also, thermal power balance can be formulated as follows:

$$P^s_{tl,pt} = \lambda_{chp,p} P^s_{echp,p} + P^s_{bil,pt} + P^s_{ts,pt} - P^s_{sur,pt}$$
$$P^s_{sur,pt} \geq 0 \quad (25)$$

D. Objective function

The objective function maximizes VPP total profit. To this aim, following profits have been taken into account:

a) Energy sales and purchasing cost at PCC_i

In each VPP unit, profit and cost from energy sale and purchase (Cpcci) depend on exchanged power at PCCi and energy sale and purchase price.

$$P^s_{\text{int},pt} > 0 \Rightarrow C^s_{pcci,pt} = \delta c_{es,h} P^s_{\text{int},pt}$$
$$P^s_{\text{int},pt} < 0 \Rightarrow C^s_{pcci,pt} = \delta c_{ep,h} P^s_{\text{int},pt} \quad (26)$$

b) ENCOURAGING PROFIT FOR RES UNIT

In PCC_e , power generated by external RES (ERES) will include the following profit (C_{PCC_e}) if it is fully sold to network:

$$C^s_{pcce,pt} = \delta c_{eres,h} P^s_{eres,pt} \quad (27)$$

In addition, internal RES (IRES) will receive following profit if either its generated power is sold to utility or consumed by internal loads:

$$C^s_{icce,pt} = \delta c_{ires,h} P^s_{ires,pt} \quad (28)$$

c) Fuel cost

Fuel cost for power generation (cgg,h) is lower than cost for thermal power generation (cgh,h) due to taxes [30]. Fuel cost per (cttc) per unit p and time t is calculated through the following equation:

$$C^s_{ttc,pt} = C_{boil,pt} P^s_{boil,pt} + C_{chp,pt} P^s_{echp,pt} \quad (29)$$

$$C_{boil,pt} = -\frac{\delta}{\eta_{boil,p}} f_{boil}\left(C_{gh,h}\right) \quad (30)$$

$$C_{chp,pt} = -\delta f_{chp}\left(C_{gh,h}, C_{gg,h}\right) \quad (31)$$

In aforementioned equations, f_{boil} converts $C_{gh,h}$ to cost, while f_{chp} considers both $C_{gh,h}$ and $C_{gg,h}$ in order to avoid considering taxes for CHP unit in current tariff framework. Start-up costs are generally considered for large thermal power generation units, while it is negligible for small CHPs.

d) Cost of risk

Preplanned and intentional load shedding has heavy fines. In order to avoid such outcomes, this cost is formulated as follows:

$$C^s_{sens,pt} = -\delta C_{sens,\text{h}} P^s_{sens,pt} \quad (32)$$

During programming for units, the algorithm may plan an intentional load shedding only when the network is operated in islanded mode and network generated power does not meet all demands.

e) Objective function final form

Final profit earned from all units' operation during total time period of generation plan is indicated as follows:

$$\zeta = \max \sum_{u=Ts}^{Te}\sum_{h=1}^{Np}\left(C^s_{pcc_i,hu} + C^s_{pcc_e,hu} + C^s_{ires,hu} + C^s_{ttc,hu} + C^s_{sens,hu}\right) \quad (33)$$

i) Uncertainty model in demand

In recent years, a large number of methods have been used in order to model uncertainty due to DERs application as well as consumption uncertainty especially in distribution level. Among these methods are Monte Carlo-, Classic clustering-, and Fuzzy-based algorithms. Probability or decision-tree method can be very effective when parameters with uncertainty are determined exactly. This method can be based on results, like results from clustering method. Ease of implementation is one of this method's advantages [31]. In this paper, consumption demand level uncertainty in electrical systems was simulated based on this method [31].

In order to model consumer load uncertainty, different methods have been presented for expected load percentage, estimated calculation and corresponding probabilities. Clustering is one of the most well-known methods, which can be planned weekly, monthly, or annually. In this work, load uncertainty was discretely modeled and probability tree method was used to generate load uncertainty scenarios [31]. Based on presented scenarios, VPP load demand is described in

Table 2. As shown in this table, hourly probabilities are

divided into two 12-hour periods, each of which has been assigned to various probabilities. Regarding previous researches in load anticipation, the highest probability (0.6) is assigned to the most exact anticipation (100%), while other anticipations have been modeled via lower probabilities.

Table 2. Discrete probability values for 24 hours ahead

Scenario Number	Probability	Expected load (Hours 1-12)	Expected load (Hours 13-24)
1	0.6	100 %	100 %
2	0.15	98.5 %	98 %
3	0.15	102 %	103 %
4	0.05	98 %	97 %
5	0.05	103 %	104 %

In this work, similar probability level for various load types were considered in all regions. This means, proposed probability structure in Table 2 is taken into account both for electrical and thermal loads. Although this assumption is not close to reality, since patterns and electrical and thermal load levels are different in microgrids, it is considered for simulation simplicity.

III. Swarm Robotics Search & Rescue optimization

During recent years, beside the methods based on mixed integer programing (MIP) [32]-[35], several heuristic methods have been developed along with the advancements of large-scale soft computing. In this paper, a recently developed evolutionary algorithm called "Swarm Robotics Search & Rescue (SRSR)" has been employed for optimization obligation [36]. Flowchart depicted in Fig. 3 shows the procedure of algorithm implementation. As opposed to the previous nature-inspired algorithms, SRSR is inspired by artificial intelligence of robots in cognitive swarm robotics. Details of optimization algorithm are provided in [36].

IV. Simulation and results

In this work, a multi-zonal VPP including five regions was studied. Based on [32] and [38], incentive value for photovoltaic generation unit is 400$ per megawatt. However, this amount is 350$ /MW for wind power generation unit. Also referring to [39] and [40] load loss cost is 8$ per kilowatt. Table 3 describes structural details of each VPP. System data is based on [23]. To model vehicles' behavior, Monte Carlo simulation has been used in each studied scenario. Average and standard deviation for daily travelled distance of PHEVs are assumed 33 and 20.4 miles, respectively [28]. In this paper, level 2 of chargers was used according to Table 1. It is assumed that in each of five VPPs, due to limitations in charger number and vehicle plug-in technology, it is possible to connect utmost 15 vehicles. It should be also noted that regarding uncertainty of vehicles' presence in operation hour, some of them are not accessible.

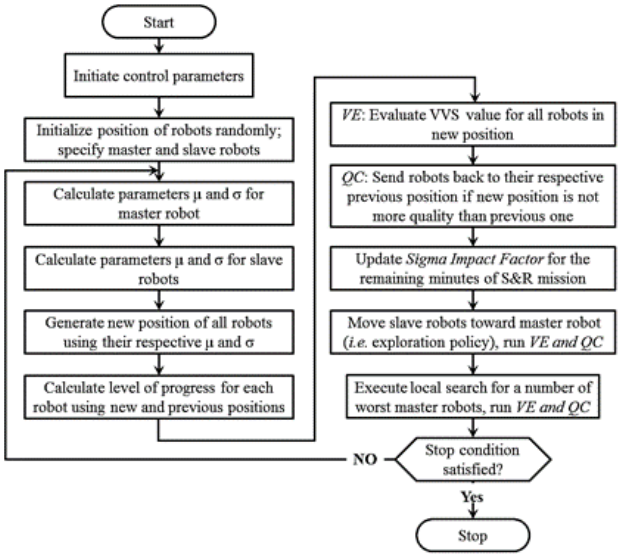

Fig. 3. Flow chart of the proposed SRSR algorithm

Table 4 shows market specifications and consumption demand for each VPP in a 24-hour time horizon. In case studies of this work, gas cost for thermal- $C_{gh,h}$ and electrical-power generation $C_{gg,h}$ are considered 0.368$/m3 and 0.349$/m3, respectively [23]. Fuel cost functions for CHPs are as follow:

$$f_{chp}\left(C_{gh,h},C_{gg,h}\right)=C_{gh,h}\frac{860}{\eta_{chp,p}LHV}+\min\left(0.25,\frac{860}{\eta_{chp,p}LHV}\right)\left(C_{gg,h}-C_{gh,h}\right) \quad (34)$$

where lower heating value (LHV) for natural gas is 8250 Kcal/m^3. Also, 860 is kWh to kcal conversion ratio.

In this research, 1/4 of delivered gas for CHP was tax-free. This means one fourth of delivered gas will be used for electrical- and the remaining will be used for thermal-power generation. Simplified function for boiler fuel cost is also presented as:

$$f_{boil}\left(C_{gh,h}\right)=\frac{860}{LHV}C_{gh,h} \quad (35)$$

Referring to [32] and [38], incentive value for photovoltaic generation unit is 400$ per megawatt. This amount is 350$ /MW for wind power generation unit. Also referring to [39] and [40], load loss cost is 8$ per kilowatt. Two various case studies, including grid-connected and islanded operation, have been done in this work.

A. Case study 1: grid-connected operation

In this case, in addition to presented operation objectives in previous section, limitations associated with transmission lines are also considered. It is expected that in peak hours, VPP uses market transactions as well as VPP's generating units and storages in order to reduce costs, increase benefit and solve the peak-shaving problem.

Fig.4- Fig. 8 show the results related to operation status of various units for each VPP.F shows scheduled generation of CHP in 24-hour period in five regions. As expected, during last hours of night, where energy market price is low, each region meets a part or all of its demand from the market. Presence of CHP results in small generators' efficiency increase, as well as it reduces natural gas purchase cost for boiler. At the hours when upstream network electricity price is low, each region purchasing electrical power from utility consumes part of it and stores the remaining in storage devices; otherwise, each region uses internal resources when utility electricity price is high, and sells surplus electrical power to utility and hence reduces its consumer costs.

Table 3. Structural data for generation units, storages, and transmission lines

	Unit 1	Unit 2	Unit 3	Unit 4	Unit 5
$P_{ech-\max}$[Kw]	50	80	80	90	150
$P_{ech-\min}$[Kw]	5	10	20	55	20
η_{chp}[%]	30	33	25	33	45
λ	1.5	0.7	1.1	0.9	1
$P_{es-char}$[Kw]	7	5	1	5	1
$P_{es-disc}$[Kw]	7	5	1	5	1
$P_{es-\max}$[Kwh]	30	60	10	20	30
$P_{es-\min}$[Kwh]	10	20	0	0	4
$P_{es-start}$[Kwh]	18	60	0	20	7
$P_{ts-char}$[Kw]	5	10	5	5	7
$P_{ts-disc}$[Kw]	5	10	5	5	7
$P_{ts-\max}$[Kwh]	40	70	20	40	30
$P_{ts-\min}$[Kwh]	10	5	5	0	3
$P_{ts-start}$[Kwh]	20	50	10	40	10
η_{boil}[%]	85	95	90	85	93
$P_{lin-\max}$[Kw]	500	500	150	500	500

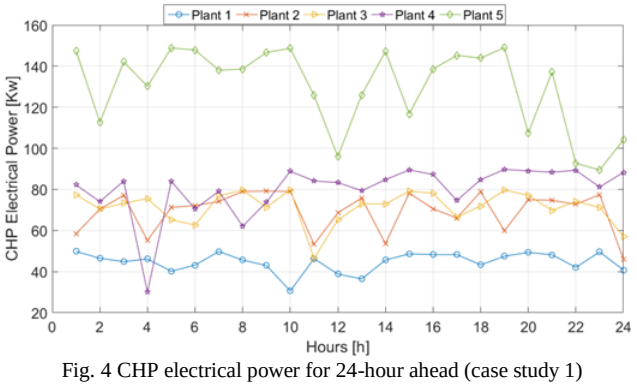

Fig. 4 CHP electrical power for 24-hour ahead (case study 1)

Table 4. Electrical and thermal consumed and RES generated power price

Hour	Purchase price	Sale price	Plant 1				Plant 2				Plant 3				Plant 4				Plant 5			
			El. load	Th. Load	IRES	ERES	El. load	Th. load	IRES	ERES	El. load	Th. load	IRES	ERES	El. load	Th. Load	IRES	ERES	El. load	Th. load	IRES	ERES
1	106	63	156	99	0	0	121	0	0	0	107	33	0	11	32	60	0	0	140	0	0	6
2	106	53	132	99	0	0	86	0	0	0	99	33	0	7	67	60	0	0	135	0	0	2
3	106	51	110	99	0	1	98	0	0	0	112	33	0	0	78	59	0	0	112	0	0	4
4	106	50	110	99	0	0	73	0	0	0	110	33	0	0	67	60	0	0	89	0	0	1
5	106	51	140	99	0	6	74	0	0	0	145	33	0	2	44	60	0	0	101	0	0	0
6	106	52	104	100	0	6	93	0	0	3	145	33	0	7	54	60	0	1	78	0	0	0
7	106	63	167	92	2	0	84	2	2	0	89	34	3	2	68	59	3	0	131	2	2	0
8	125	67	156	84	5	2	104	98	5	6	134	35	5	4	104	60	5	1	129	79	5	0
9	135	73	184	10	2	2	121	112	9	3	105	50	10	7	57	60	11	0	149	86	11	1
10	135	80	219	88	2	6	146	105	2	0	120	61	2	7	123	59	3	4	123	71	3	0
11	135	80	208	88	7	4	175	117	6	0	132	68	8	2	109	59	7	1	152	90	7	1
12	135	80	177	83	11	13	178	100	11	0	169	70	12	2	87	59	11	4	106	75	13	0
13	135	70	113	92	14	6	105	86	12	10	122	70	15	0	62	59	12	4	137	1	15	1
14	135	69	156	97	11	9	133	117	12	16	154	65	11	24	84	60	11	4	125	0	13	0
15	135	73	123	97	7	13	150	105	6	0	107	65	8	0	88	60	7	4	108	2	7	0
16	135	79	207	97	2	9	148	115	2	3	142	68	2	0	63	60	3	24	126	22	2	0
17	135	80	217	97	24	2	172	117	24	3	151	67	24	0	96	60	24	17	134	82	24	3
18	135	71	222	95	17	24	160	112	17	24	129	58	16	0	58	59	19	11	107	83	17	0
19	135	66	204	95	10	24	119	111	10	3	137	50	11	0	67	59	10	4	133	83	10	6
20	125	67	193	95	5	4	115	102	5	16	132	40	5	0	76	59	5	4	113	68	5	6
21	125	72	141	96	2	4	59	2	3	16	99	44	3	1	58	59	3	4	99	2	3	13
22	125	77	86	95	0	6	48	0	0	0	96	33	0	0	56	60	0	0	132	0	0	24
23	125	67	100	94	0	2	56	0	0	0	149	32	0	0	45	60	0	0	129	0	0	17
24	106	63	99	93	0	1	55	0	0	0	93	32	0	0	56	60	0	0	87	0	0	13

It can be observed that the first unit is operated at its maximum rate in order to meet electrical demand in most of the hours. Since in most of the time, electrical demand is higher than its generating capacity, this unit keeps its generation close to maximum amount, providing the remaining from storage sources, and if it lacks power, meets the remaining using upstream utility power. For the fourth unit, this is the same from 10:00 to 16:00. The difference is that in this region, thermal load demand is uniformly high. Therefore, it is economically beneficial to use CHP instead of boiler to meet thermal loads and sell surplus electrical power to energy market, regarding higher energy purchase price. As it can be seen, met load by the fifth unit at 16:00 is at its maximum thermal and electrical amount. Since this unit has high generating capacity, its generation reaches to maximum amount. It should also be noted that, due to low market sale price (not being economical) and storage limits, the fifth unit would not generate at its maximum rate. Fig. 5 and Fig. 6 show daytime stored energy trend. Regarding storage rate limitation, storage devices are capable of storing power with known values. Also, it is assumed that in order to increase storage devices' lifetime, their end of schedule

level returns to initial level; so each region is limited not to generate its maximum power in all hours. It should be noted that VPPs' priority sequence in power generation is internal load demand, storage in limited storage devices, and finally sale to market in case of surplus power. Therefore, it is not economical for VPPs to operate CHPs in all hours in their maximum rate.

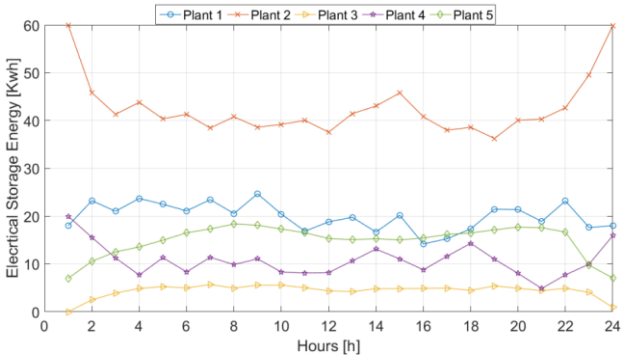

Fig. 5 Electrical charge/ discharge state for 24 hours ahead (case study 1)

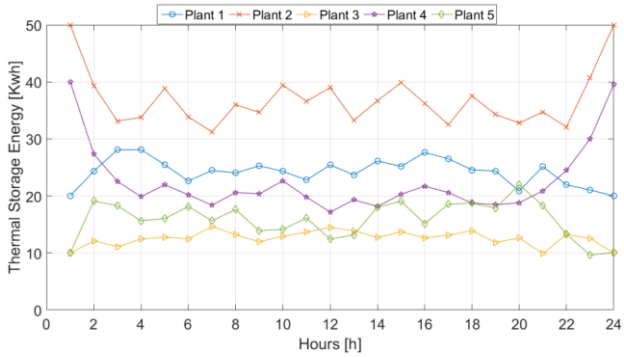

Fig. 6 Thermal charge/discharge state for 24 hours ahead (case study 1)

Depending on gas, electricity price and load patterns, RES plants' generation and technical limitations in CHPs of each region, and electrical and thermal charge/discharge cycle may be totally different. So, it is not easy to decisively investigate power changes in storages. In addition to all mentioned parameters, charge and discharge equality during an operation interval is an objective which makes the anticipation of storage device behavior even more complicated. Fig. 7 presents boiler generated thermal power procedure during daily operation period. As shown in the figure, corresponding to thermal load increment of each region from 8:00 to 20:00, boiler operation increases in mentioned time. This condition is also observable for the second unit. Regarding that in mentioned hours, thermal load of this region is much higher than CHP thermal generation as well as thermal storage device capacity; boiler presence is a necessity in order to compensate for power shortage. It should be noted that, regarding CHP and storage performance near its maximum rate during the mentioned hours, boiler performance pattern in this region exactly coincides with thermal load pattern.

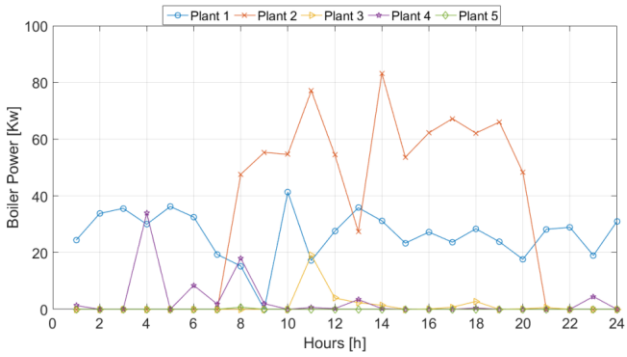

Fig. 7 Thermal power by boiler (case study 1)

For instance, this state at 13:00 hours where second region thermal load decreases dramatically for one hour, is obviously observable; therefore, the second boiler, according to this demand decrement, decreases its generation. Power flow in interface transmission lines between regions and upstream utility is shown in Fig. 8.

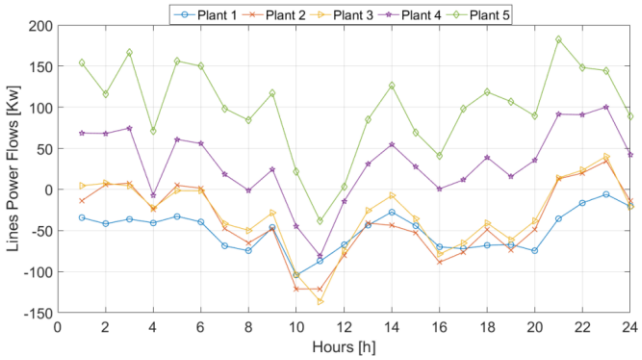

Fig. 8 Power flow of transmission line between regions (case study 1)

As shown, due to line high capacity, no line reaches its rated value. It should also be noted that, transmission line in region 3 which has lower thermal limit, reaches close to its rated capacity at 11:00 hours. Remarkable point is that power analysis in of line 5 (connected to upstream utility sub-station) show that unlike other times where upstream acts as a feeder, at 11:00 hours is seen as a load from LSVPP point of view. In this condition, VPPs are capable of selling energy to upstream network as well as feeding internal loads, and unlike other times of day, performance of photovoltaic units, CHPs' surplus generation, and electrical storage devices, reverse power flow direction in upstream connected transmission line. This direction change in power flow is also seen during different hours in other lines. Number of scheduled vehicles in 24-hour ahead operation is shown in Fig. 9.

It is shown that number of vehicles conforms to network load pattern to some extent, so that during peak time, number of recruited vehicles increases; however compared to CHPs, this conformity would not be so difficult; since, regardless of conformity to load pattern, entering time of vehicle units to parking would associate some percentage of uncertainty in the charging procedure of a smart vehicle. Also, the amount of battery charging when vehicle enters the parking will depend on factors such as travelled distance, which is a random process as well.

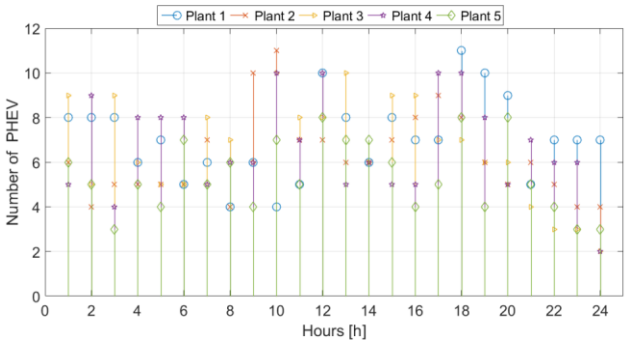

Fig. 9 Number of EVs in operation horizon (case study 1)

Total benefit earned from VPPs' operation conforms to combination of gathered energies' sales pattern and encouraging subsides from external and internal RESs as well as load pattern; while current costs' pattern is generally a combination of pattern of consumed electrical and thermal load demand as well as energy purchase price from market.

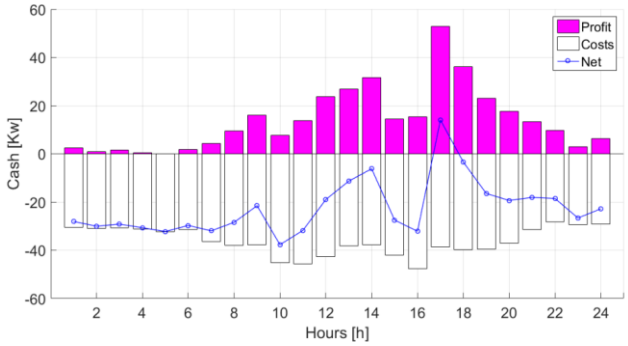

Fig. 10 LSVPP financial transaction in 24 hour ahead (case study 1)

Fig. 10 shows operation costs, earnings and profits from generation schedule. It should be noted that these relations and pattern combinations are not linear. As it is shown and also mentioned before, at 8:00 to 22:00 hours when electricity sale price is higher, each region uses its internal units in order to meet demand, so power purchased from utility decreases; therefore, operation costs reaches its minimum value due to higher generation. In this special study on VPP scheduling and planning, mathematical expectation for resulted income regarding Table 5 reached 534 dollars, which compared to the case without load uncertainty, shows 3.5% reduction [23].

Table 5. Final operation profit expectation calculation in grid-connected mode (case study 1)

	Scenario 1	Scenario 2	Scenario 3	Scenario 4	Scenario 5
Profit[$]	-520.83	-543.46	-566.08	-531.86	-584.46
Probability	0.6	0.15	0.15	0.05	0.05
Expected profit			-534.745		

B. CASE STUDY 2: ISLANDED OPERATION

In this case islanding operation of network is studied. In this case part of the network disconnects from upstream distribution network. In mentioned condition, network should keep dynamic and static stability. To this aim, LSVPP generation schedule and performance in islanded mode is one of the most important problems related to distribution network operation, which was studied in this paper. In this way, an exact schedule was prepared for islanded system operation, taking into account system reliability and adequacy. In order to execute this, it was assumed that interface transmission line between last region and upstream network substation, disconnects after an event. This is shown in Fig. 11.

Fig. 12- Fig. 16 show results regarding operation status of various elements in each VPP for current case study. In order to compare CHP units' generation power for normal operation in Fig.4 and islanded operation in Fig. 12 two points should be considered;

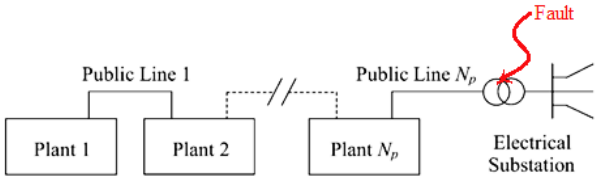

Fig. 11 Fault at final VPP connection point to upstream network

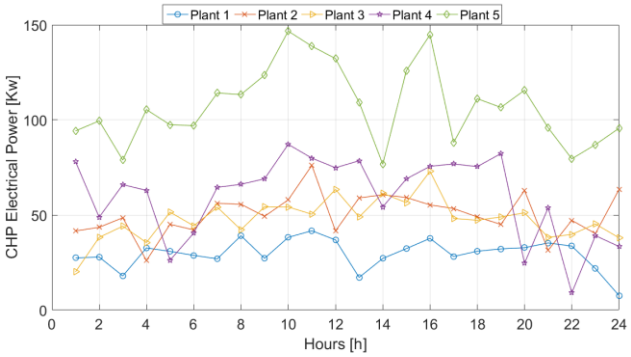

Fig. 12 CHP electrical power for 24-hour ahead (case study 2)

First, due to inability of upstream network in providing power, all units should provide electrical power and as much as possible thermal power in their own region. Therefore, generation level for some units decreases due to inability in selling surplus power to upstream network (e.g. unit five at 1:00 to 8:00 hours), and at some hours power increases due to meeting balance power objective (e.g. unit one at 7:00 to 17:00 hours). However, it should be noted that power exchange with adjacent region units is still possible. Second point is that, by comparing load pattern of each region and generative power of CHPs in that region, it is observable that CHP generation pattern conforms highly to load pattern of the same region. Noticeably, due to presence of electrical storage and power exchange possibility with adjacent regions, this will not be a definite conformity. Electrical and thermal storage charge and discharge state in LSVPP islanded mode are shown in Fig. 13 and Fig. 14, respectively

It is shown that smooth and uniform changes in charge and discharge levels of electrical storage devices, turn into sharper

changes in islanded mode in order to meet power balance objective. The reason is that charge and discharge pattern of these storages are more influenced by energy sale and purchase price pattern in normal operation mode in order to increase VPP profit, while in islanded mode this becomes the second priority since rigid network operation objectives are of higher importance in this condition. It should be noted that thermal storages does not experience these high fluctuations; since there are no thermal power transmission lines between existing regions and in this case study, most changes of thermal storages are only influenced by variation curve of CHP plants' generated thermal power. Regarding that this case study simulates special operation condition, which may occur rarely during year, 10% tolerance is allowable in storage devices' charge and discharge equality objective during the operation time.

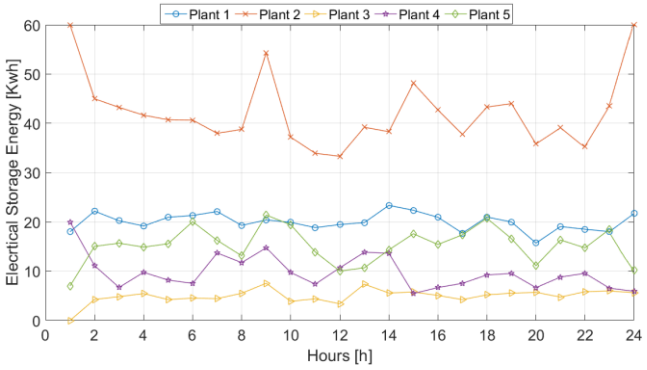

Fig. 13 Electrical storage charge and discharge state for 24 hour ahead (case study 2)

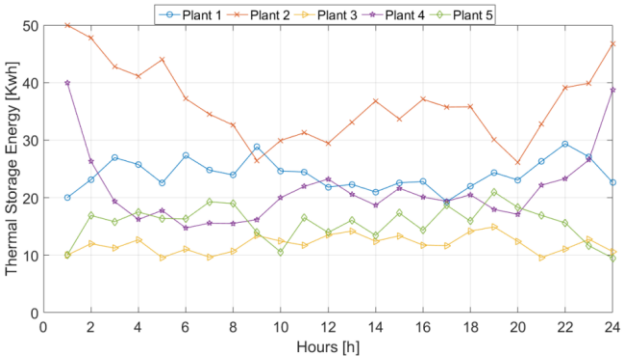

Fig. 14 Thermal storage charge and discharge state for 24 hour ahead (case study 2)

Fig. 15 shows boiler generated power. It is indicated that boiler power pattern highly conforms to thermal load demand. This is well observable in region two boilers. It should be noted that in some regions (such as region five), due to high CHP unit capacity located in this region associated with thermal storage, the main part of thermal load is fed by these two elements and aforementioned point would not be applied for this case. Power flow in transmission lines is shown in Fig. 16. Current in line ended to upstream network is zero due to an event, which is the reason of network being islanded. Compared to normal operation, it is shown that in islanded mode, current flow in most of the lines is decreased at most of the hours. This was totally expected due to VPPs disconnection from upstream network and inability of power exchange at peak hours to meet a part of demand and at low market price hours to charge batteries. Fig. 17 shows scheduled vehicle numbers for 24 hour ahead operation. Fig. 18 shows income, cost and benefit from operation of all VPPs. It is indicated that cost and income pattern is so similar to case study 1.

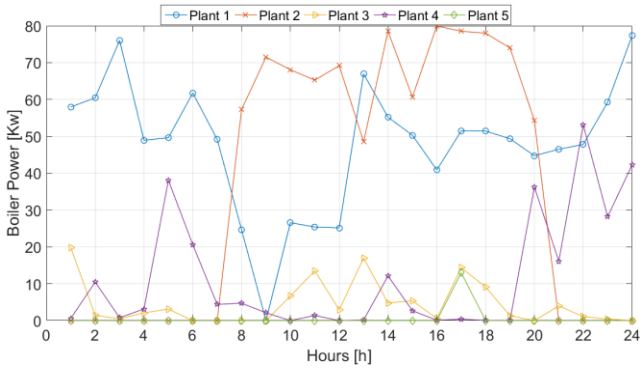

Fig. 15 Generated thermal power by boiler (case study 2)

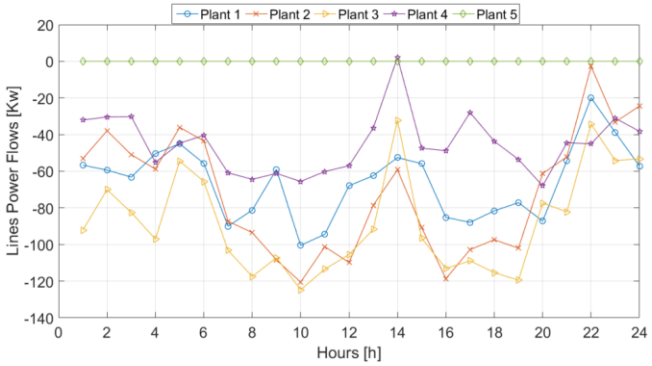

Fig. 16 Power flowing in interface transmission lines between the regions (case study 2)

Although, hourly values of these parameters have experienced some variations, transmission line disconnection from utility would not have remarkable effect on how financial transactions are done. One of the reasons is that sale and purchase price in VPP point of common coupling to adjacent units does not differ in this case study with previous one and only limitations are power shortage supply and high load shedding costs. It is shown that operation costs are also more than first case study; since more use of fuel in order to generate more power causes more operation cost. As shown, in this case study too fewer vehicles have been utilized compared to previous one. Clearly, its reason is decrease in network capacity for exchange with upstream network. In this condition of VPP scheduling and operation, regarding Table 6, mathematical expectation for resulted income reaches to about -704 dollars which is 30% lower than non-islanded operation state. It is certain that in normal operation, due to sale and purchase possibility with upstream network at hours when energy purchase price is low or when energy price is high, transaction with market will result in more profit for system operators. As shown, due to more boiler and CHP utilization, operation costs increase, while due to surplus power sales possibility to upstream network, incomes increase. It should be noted that, in islanded operation mode, since all regions have similar format, power shortage or surplus is almost

similar for all regions; therefore, either in power shortage or power surplus condition, reaching the most optimal operation condition is not possible by only exchanging power with adjacent regions, and this condition finally results in more operation cost. Comparing Table 6 and Table 8 shows that, by changing the case study, operation cost decreases from -534.745 in normal conditions to -704.832 in islanded operation. Accumulative benefit curve for two cases studies are shown in Fig. 19.

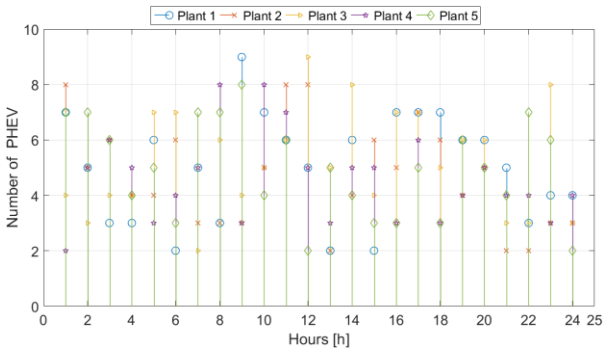

Fig. 17 Electric vehicle numbers in operation time horizon (case study 2)

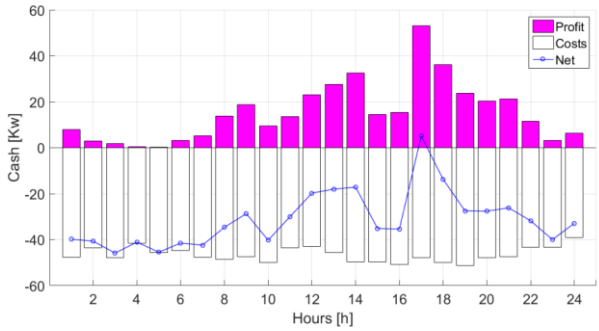

Fig. 18 LSVPP financial transaction in 24 hour ahead (case study 2)

Table 6. Final operation benefit expectation calculation in islanded operation (case study 2)

	Scenario 1	Scenario 2	Scenario 3	Scenario 4	Scenario 5
[$] Profit	-707.17	-666.85	-718.93	-653.70	-799.58
Probability	0.6	0.15	0.15	0.05	0.05
Expected profit			-704.832		

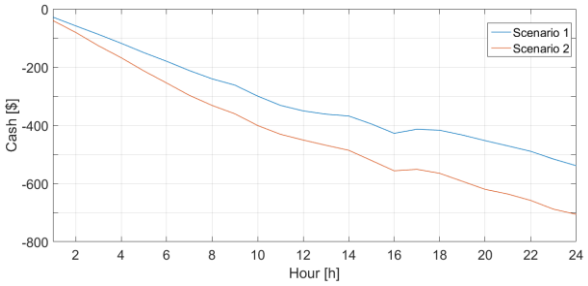

Fig. 19 Accumulative benefit cash flows.

V. CONCLUSION

In this paper, an optimal scheduling for LSVPP including multiple regions was presented. Small VPPs were assumed similar and connected to each other via transmission lines, while the last unit was connected to upstream distribution network substation. Each unit had RESs, storages (thermal and electrical), CHPs and parking lot. The objective function of network operation aimed at maximizing total VPPs benefit as well as meeting thermal and electrical demand. Optimization was done by an evolutionary algorithm and electrical load uncertainty was modeled by scenarios based on discrete probability distribution and mathematical expectation, while vehicle behavior uncertainty was modeled using Monte Carlo simulation. Two case studies, normal operation and islanded operation, were considered and state of each element in VPP were presented and analyzed via their performance curves in a 24 hour day-ahead period. It was shown that taking into account load uncertainty compared to basic case, decreased costs, while islanded operation caused increase in system operation costs. It should also be noted that islanded operation occurred only in rare and special cases and in short periods.

EFERENCES

[1] Yavuz, L., Önen, A., Muyeen, S. M., & Kamwa, I. (2019). Transformation of microgrid to virtual power plant–a comprehensive review. IET Generation, Transmission & Distribution, 13(11), 1994-2005.

[2] Nosratabadi, S. M., Hooshmand, R. A., & Gholipour, E. (2017). A comprehensive review on microgrid and virtual power plant concepts employed for distributed energy resources scheduling in power systems. Renewable and Sustainable Energy Reviews, 67, 341-363.

[3] Nguyen, H. T., Le, L. B., & Wang, Z. (2018). A bidding strategy for virtual power plants with the intraday demand response exchange market using the stochastic programming. IEEE Transactions on Industry Applications, 54(4), 3044-3055.

[4] Kabalci, Y. (2016). A survey on smart metering and smart grid communication. Renewable and Sustainable Energy Reviews, 57, 302-318.

[5] Vanhoudt, D., Claessens, B. J., Salenbien, R., & Desmedt, J. (2018). An active control strategy for district heating networks and the effect of different thermal energy storage configurations. Energy and Buildings, 158, 1317-1327.

[6] Kardakos, E. G., Simoglou, C. K., & Bakirtzis, A. G. (2015). Optimal offering strategy of a virtual power plant: A stochastic bi-level approach. IEEE Transactions on Smart Grid, 7(2), 794-806.

[7] Braun, M. (2007). Technological control capabilities of DER to provide future ancillary services. International journal of distributed energy resources, 3(3), 191-206.

[8] Lombardi, P., Stötzer, M., Styczynski, Z., & Orths, A. (2011, July). Multi-criteria optimization of an energy storage system within a Virtual Power Plant architecture. In 2011 IEEE Power and Energy Society General Meeting (pp. 1-6). IEEE.

[9] Li, H., Tan, Z., Chen, H., & Guo, H. (2018). Integrated heat and power dispatch model for wind-CHP system with solid heat storage device based on robust stochastic theory. Wuhan University Journal of Natural Sciences, 23(1), 31-42.

[10] Ramsay, C. and Aunedi, M., "Characterisation of LSVPPs", Fenix project, Del. D1.4.1. [Online]. Available: http://fenix.iwes.fraunhofer. de/html/documents.htm

[11] Vanhoudt, D., Claessens, B. J., Salenbien, R., & Desmedt, J. (2018). An active control strategy for district heating networks and the effect of different thermal energy storage configurations. *Energy and Buildings*, *158*, 1317-1327.

[12] Zdrilić, M., Pandžić, H., & Kuzle, I. (2011, May). The mixed-integer linear optimization model of virtual power plant operation. In *2011 8th International Conference on the European Energy Market (EEM)* (pp. 467-471). IEEE.

[13] Zamani, A. G., Zakariazadeh, A., Jadid, S., & Kazemi, A. (2016). Stochastic operational scheduling of distributed energy resources in a large scale virtual power plant. *International Journal of Electrical Power & Energy Systems*, *82*, 608-620.

[14] Kuzle, I., Zdrilić, M., & Pandžić, H. (2011, May). Virtual power plant dispatch optimization using linear programming. In *2011 10th International Conference on Environment and Electrical Engineering* (pp. 1-4). IEEE.

[15] Ruiz, N., Cobelo, I., & Oyarzabal, J. (2009). A direct load control model for virtual power plant management. *IEEE Transactions on Power Systems*, *24*(2), 959-966.

[16] Caldon, R., Patria, A. R., & Turri, R. (2004, September). Optimisation algorithm for a virtual power plant operation. In *39th International Universities Power Engineering Conference, 2004. UPEC 2004.* (Vol. 3, pp. 1058-1062). IEEE.

[17] Maanavi, M., Najafi, A., Godina, R., Mahmoudian, M., & MG Rodrigues, E. (2019). Energy Management of Virtual Power Plant Considering Distributed Generation Sizing and Pricing. *Applied Sciences*, *9*(14), 2817.

[18] Okpako, O., Rajamani, H. S., Pillai, P., Anuebunwa, U., & Swarup, K. S. (2017, September). A Comparative Assessment of Embedded Energy Storage and Electric Vehicle Integration in a Community Virtual Power Plant. In *International Conference on Wireless and Satellite Systems* (pp. 127-141). Springer, Cham.

[19] Wang, M., Mu, Y., Jia, H., Wu, J., Yu, X., & Qi, Y. (2017). Active power regulation for large-scale wind farms through an efficient power plant model of electric vehicles. *Applied Energy*, *185*, 1673-1683.

[20] Ju, L., Li, H., Zhao, J., Chen, K., Tan, Q., & Tan, Z. (2016). Multi-objective stochastic scheduling optimization model for connecting a virtual power plant to wind-photovoltaic-electric vehicles considering uncertainties and demand response. *Energy Conversion and Management*, *128*, 160-177.

[21] Rostami, M. A., & Raoofat, M. (2016). Optimal operating strategy of virtual power plant considering plug-in hybrid electric vehicles load. *International Transactions on Electrical Energy Systems*, *26*(2), 236-252.

[22] Kahlen, M., & Ketter, W. (2015, February). Aggregating electric cars to sustainable virtual power plants: The value of flexibility in future electricity markets. In *Twenty-Ninth AAAI Conference on Artificial Intelligence*.

[23] Giuntoli, M., & Poli, D. (2013). Optimized thermal and electrical scheduling of a large scale virtual power plant in the presence of energy storages. *IEEE Transactions on Smart Grid*, *4*(2), 942-955.

[24] "World Wind Energy Association- Press Release", http://www.wwindea.org,Feb.2009.

[25] Barsali, S., Ceraolo, M., Giglioli, R., & Poli, D. (2003, June). Aggregation and management of the demand in a deregulated electricity market. In *2003 IEEE Bologna Power Tech Conference Proceedings*, (Vol. 4, pp. 4-pp). IEEE.

[26] Barsali, S., Bechini, A., Giglioli, R., & Poli, D. (2012, September). Storage in electrified transport systems. In *2012 IEEE International Energy Conference and Exhibition (ENERGYCON)* (pp. 1003-1008). IEEE.

[27] Qian, K., Zhou, C., Allan, M., & Yuan, Y. (2010). Modeling of load demand due to EV battery charging in distribution systems. *IEEE transactions on power systems*, *26*(2), 802-810.

[28] Li, G., & Zhang, X. P. (2012). Modeling of plug-in hybrid electric vehicle charging demand in probabilistic power flow calculations. *IEEE Transactions on Smart Grid*, *3*(1), 492-499.

[29] Rezaee, S., Farjah, E., & Khorramdel, B. (2013). Probabilistic analysis of plug-in electric vehicles impact on electrical grid through homes and parking lots. *IEEE Transactions on Sustainable Energy*, *4*(4), 1024-1033.

[30] Dulău, L. I., Abrudean, M., & Bică, D. (2014, September). Distributed generation and virtual power plants. In *2014 49th International Universities Power Engineering Conference (UPEC)* (pp. 1-5). IEEE.

[31] Saber, A. Y., & Venayagamoorthy, G. K. (2011). Resource scheduling under uncertainty in a smart grid with renewables and plug-in vehicles. *IEEE systems journal*, *6*(1), 103-109.

[32] Vanderbei, R. J. (2020). *Linear programming: foundations and extensions* (Vol. 285). Springer Nature.

[33] Wong, J. Y. (2014). Testing the Nonlinear Integer Programming Solver Here with Generalized Euler Bricks.

[34] Alemany, J., Magnago, F., Moitre, D., & Pinto, H. (2014). Symmetry issues in mixed integer programming based Unit Commitment. *International Journal of Electrical Power & Energy Systems*, *54*, 86-90.

[35] Gil, E., Aravena, I., & Cárdenas, R. (2014). Generation capacity expansion planning under hydro uncertainty using stochastic mixed integer programming and scenario reduction. *IEEE Transactions on Power Systems*, *30*(4), 1838-1847.

[36] Bakhshipour, M., Ghadi, M. J., & Namdari, F. (2017). Swarm robotics search & rescue: A novel artificial intelligence-inspired optimization approach. *Applied Soft Computing*, *57*, 708-726.

[37] Italy4th Conto Energia (Summary), May 2011, European Photovoltaic Industry Association.

[38] ItalyAnnual Report, Aug. 2011, International Energy Agency Wind.

[39] Kariuki, K. K., & Allan, R. N. (1996). Evaluation of reliability worth and value of lost load. *IEE proceedings-Generation, transmission and distribution*, *143*(2), 171-180.

[40] Li, W. (2006). Expected Energy Not Served (EENS) Study for Vancouver Island Transmission Reinforcement Project. *Report-BCTC*.